ISSN 1061-933X, Colloid Journal, 2015, Vol. 77, No. 6, pp. 770–779. © Pleiades Publishing, Ltd., 2015.
Original Russian Text © S.P. Molchanov, V.I. Roldughin, I.A. Chernova-Kharaeva, 2015, published in Kolloidnyi Zhurnal, 2015, Vol. 77, No. 6, pp. 764–774.

Three Scenarios of Evaporation of Microliter Droplets of Dispersions and Structure of Formed Ring-Shaped Deposits

S. P. Molchanov[a], V. I. Roldughin[b], and I. A. Chernova-Kharaeva[a]

[a] *Photochemistry Center, Russian Academy of Sciences, ul. Novatorov 7a, bldg. 1, Moscow, 119421 Russia*
e-mail: spmolchanov@mail.ru

[b] *Frumkin Institute of Physical Chemistry and Electrochemistry, Russian Academy of Sciences, Leninskii pr. 31, Moscow, 119071 Russia*
e-mail: vroldugin@yandex.ru

Received April 23, 2015

Abstract—Experiments have been performed on the formation of ring-shaped deposits by evaporating droplets of dispersions using the coffee ring effect. The experiments have been carried out with aqueous dispersions of polystyrene and silica submicron particles, as well as SiO_2 particles of the Levasil brand with a size of 50 nm. It has been shown that there are three different scenarios of deposit formation and droplet meniscus displacement. The deposits may be formed as rings and disks. When ring-shaped deposits are formed, the displacement of the meniscus may be essentially different (from the periphery to the center of the droplet and vice versa) depending on the nature of particles. The mechanisms responsible for the realization of different scenarios have been considered at the qualitative level.

DOI: 10.1134/S1061933X15060162

INTRODUCTION

Evaporation of free droplets and sessile droplets on substrates are the subjects of numerous theoretical and experimental investigations [1–4], because the droplet evaporation accompanies various natural and technological processes, while many fundamental problems relevant to the evaporation still remain unsolved. Droplet evaporation is involved in spray drying and used in medicine (inhalation), in heat exchangers, etc. Evaporation/condensation processes govern the dynamics of clouds and fogs.

Sessile droplet evaporation accompanies the application of substances—in particular, pesticides—onto solid substrates. It predetermines the quality of printing in inkjet printers. Evaporation of dispersion droplets is an unavoidable stage of the formation of photon crystals [5, 6] and ordered structures from DNA and RNA macromolecules on substrates [7]. The performed investigations have shown a strong influence of droplet size and composition on the evaporation process (see [8]).

Works [9, 10] induced great interest in the study of the evaporation of sessile droplets of dispersions and solutions, during which a deposit of a dissolved substance is formed along the perimeter of a droplet (coffee ring effect, CRE). The deposition of dissolved substances has been shown to occur via a rather complex mechanism involving convective motion, which is caused by nonuniform temperature, and the Marangoni effect. This circumstance has induced additional interest in the investigation of heat effects. In particular, it has been theoretically and experimentally shown [11–13] that these effects are strongly influenced by the nature of a substrate, more exactly, its heat conductivity. The influence of the nature of a substrate on the structure of a deposit was also mentioned in [14–17], where variations in the structure of a deposit was related to variations in the hydrophilic/hydrophobic properties of a substrate. The role of these properties was also mentioned in our previous work [18], where we have obviously demonstrated variations in the structure of a deposit formed by the CRE mechanism occurring due to variations in initial contact angles, because the same substrates treated in different manners were used in experiments. Moreover, the main factors affecting the initial contact angles of dispersion droplets were found out in [18], with the deposit structure being, in the long run, dependent on the contact angle.

The important role of the contact angle in the formation of the deposit structure was noted in [19], where the evaporation of a sessile droplet was numerically simulated. In the course of the simulation, the diffusion of particles, heat effects, Marangoni convection, and displacement of the three-phase contact line were taken into account. It was assumed that the displacement of the three-phase contact line (depinning) begins when particle concentration in the region of the meniscus reaches a value corresponding to the dense packing, or the receding contact angle becomes

smaller than some limiting value. It was shown that, depending on the value of this limiting contact angle, two scenarios of droplet evaporation and deposit formation ("from the perimeter to the center" and "from the center to the perimeter") may take place. At a rather large limiting angle, a droplet evaporates "from the perimeter to the center." On the contrary, at a small receding angle, the droplet is, as it were, evaporating in the regime "from the center to the perimeter." The authors of [19] also reported the results of their own experiments, which confirmed the main features of a deposit structure and, therefore, were used as grounds for consideration of this model as adequate for real processes. At the same time, as can be seen from the data reported in [19], the deposits formed in the experiments had a nontrivial structure, which was not reproduced by numerical simulation and indicated an incompleteness of the scenarios proposed in that work for droplet evaporation.

In this work, we shall present some results of studying a large number of systems, which indicate that the number of scenarios for evaporating dispersion droplets is, in fact, larger. In particular, new regularities will be shown for the displacement of the three-phase contact line and variations in the shape of a droplet during its evaporation. Note that the process of droplet evaporation was not studied in [19], and the authors confined themselves to the comparison between the simulation data and the structures formed at the final stage. Our monitoring of variations in the shape of a droplet with time shows that, with regard to the receding contact angle, a droplet does not, in reality, evaporate in accordance with the scenarios proposed in [19]. Therewith, the depinning begins for reasons other than those mentioned in [19]. The mechanisms of depinning will be described in detail in our subsequent work. Here, we shall, without going into details of solid deposit formation, describe different scenarios of variations in the shapes of evaporating droplets and resulting deposits for three different dispersions, with these scenarios being typical of all systems that we have experimentally studied (including many-ring structures, because each ring is formed in them via one of the proposed scenarios). The experimental data that are characterized by insubstantial variations in the basic scenarios are not presented in this article because of its limited volume.

EXPERIMENTAL

Experiments were performed with dispersion droplets obtained using Lenpipet Digital dosing pipettes enabling one to apply droplets with volumes of 10–100 or 2–10 μL on a substrate. Deionized water, which was obtained by sorption and ion-exchange filtration followed by mechanical microfiltration in a D-301 deionizer (Akvilon, Russia), and dispersions prepared in it were used in the experiments. We used aqueous 5 wt % dispersions of polystyrene and SiO_2 microsized particles 250 and 255 nm in diameter, respectively (below, the latter are referred to as "silica particles"), as well as SiO_2 nanoparticles with a diameter of 50 nm (Levasil, H.C. Starck, Inc.).

Contact angles of droplets of different dispersions with a particle concentration of 5 wt %

Evaporation scenario	I	II	III
Dispersed phase	Polystyrene	Silica	Levasil
Initial contact angle, deg	31	30	34
Depinning angle, deg	31	26	18
Depinning time	0	8	90

Menzel-Gläser microscope slides with sizes of 75 × 25 × 1 mm^3 were used as hydrophilic substrates, the surface of which was cleaned as follows: a slide was exposed in 2-propanol, which had been filtered through a 5-μm filter, for 1 h; washed with a large amount of 2-propanol; and dried in a Spincoater P6700 setup (Specialty Coating Systems, United States). Computer disks, the working surface of which had a protective coating of a fluoroorganic polymer, were used as hydrophobic substrates.

The droplets were monitored and the contact angles were measured using an optical video stand (Photochemistry Center, Russian Academy of Sciences) [20], assembled from a measuring table with a substrate, onto which a droplet was applied, and vertical and horizontal microscopes equipped with video cameras, which monitored the droplet under different angles.

EVAPORATION OF PURE WATER DROPLETS

Hydrophilic Substrate

It made perfect sense to begin the analysis of the scenarios of evaporating dispersion droplets from studying the evaporation of particle-free solvent droplets. We carried out experiments on the evaporation of deionized water droplets with volumes of 2–10 μL applied onto a microscope slide with a dosing pipette (initial contact angle of 33°). Variations in the parameters of a droplet were monitored with the use of the optical video stand (by taking top- and side-view micrographs). The contact angle was measured at intervals of 180 s. Note that, as we had shown previously [18], within the experiment error, the initial contact angle is independent of the droplet volume in the aforementioned range of its variations.

Figure 1 depicts a 7-μL droplet in different time intervals after the onset of evaporation (side view),

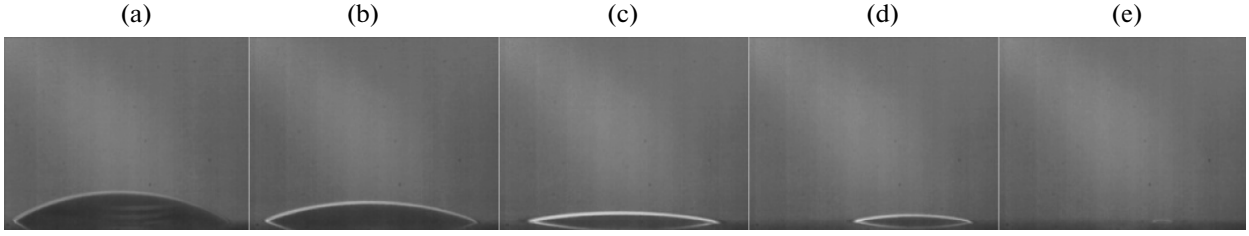

Fig. 1. Evaporating 7-μL droplet of deionized water photographed at different time moments with intervals of 720 s.

while Fig. 2 shows the time dependences of the contact angle and relative radius of the contact spot (r/r_0, where r is the current radius and r_0 is the initial droplet radius) for this droplet. Analogous dependences were observed for droplets of other volumes.

Let us pay attention to the fact that, at the initial stage, the droplets are evaporated at fixed areas of their bases (i.e., pinning takes place). Only the contact angle varies (decreases). When the contact angle reaches the value of the receding contact angle, meniscus displacement (depinning) begins. The fixation of the three-phase contact line (pinning) is of fundamental importance for the formation of ring-shaped structures. The determination of this mechanism requires special experimental investigations, the results of which are intended to be represented later on.

Hydrophobic Substrate

Analogous experiments were performed for a hydrophobic substrate (the surface of a compact disk), on which the initial contact angle of a water droplet was nearly 80°. Not that, in this case, droplets with different volumes also exhibit almost the same behavior; however, it essentially differs from the behavior of the droplets on the hydrophilic substrate. Micrographs taken from a 7-μL droplet at different moments of time with intervals of 380 s (side view) are shown in Fig. 3, while Fig. 4 illustrates the time dependences of

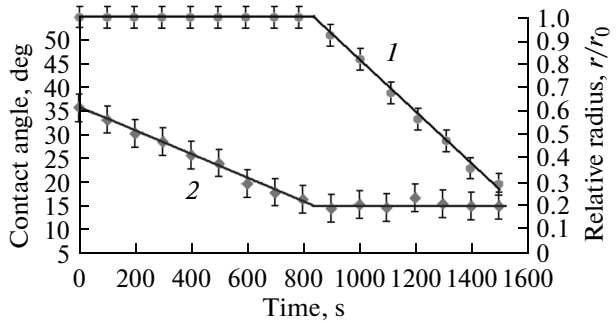

Fig. 2. Time dependences of (*1*) relative radius and (*2*) contact angle of a 7-μL water droplet on a hydrophilic substrate.

the contact angle and relative radius of the contact spot for this particle.

Comparison of Figs. 1, 2 and 3, 4 shows an essential difference between the behaviors of the droplets on hydrophilic and hydrophobic surfaces. For hydrophilic surfaces, the pinning phenomenon takes place, while the depinning begins later on. On hydrophobic surfaces, the three-phase contact line displacement begins immediately, while its fixation is observed only at the final stage. Accordingly, at the initial stage, the droplet on the hydrophilic surface evaporates "at an unchanged radius," while, on the hydrophobic surface, the initial stage of droplet evaporation occurs "at an unchanged shape."

These data once more emphasize the complex mechanism of droplet evaporation on solid substrates: even in the case of pure water, the character of the three-phase contact line displacement is nontrivial. The situation becomes substantially more complex for the evaporation of dispersion droplets.

EVAPORATION OF DISPERSION DROPLETS

Droplets of aqueous 5% dispersions of polystyrene, silica, and Levasil with the same volume equal to 40 μL were dried on the same substrate under the same external conditions. Immediately after a droplet was applied, the evaporation process was monitored by taking micrographs (top and side views) with intervals of 1 s. The equilibrium contact angles were measured in the micrographs immediately after the droplets were applied onto a substrate (initial contact angles) and at the moment of the onset of the wetting line displacement to the center (depinning angles). The time elapsed from the droplet application to the onset of meniscus displacement (depinning time) was determined. In addition, the radii of the droplets (distances from the droplet center to the three-phase contact line) at different moments of time and the profiles of solid deposits along a spot radius were determined.

Dispersions of Polystyrene Particles

Figure 5 shows the top-view micrographs taken from an evaporating droplet of a dispersion of polystyrene particles at different time moments. Figure 6 presents the time dependences of relative external and

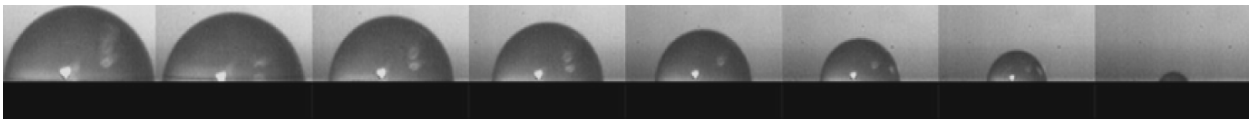

Fig. 3. Evaporating 7-μL water droplet photographed at different time moments with intervals of 380 s after the onset of evaporating.

internal radii of a droplet. The droplet evaporates in the following way. After it is applied and the equilibrium state is established (Fig. 5a), the displacement of the droplet external boundary from the periphery to the center over the formed solid deposit (depinning) immediately begins. The displacement of the external boundary decelerates, because the thickness of the fringe grows, and an increasing amount of particles are obviously required for a rise in its thickness. In some period of time, the fringe is formed almost completely (Fig. 5b), and the three-phase contact line ceases to move. More detailed studies have shown that the three-phase contact line does not stop moving and the formation of the deposit fringe permanently goes on, being limited by the influx of particles and depending on the current shape of a droplet. In the subsequent works, it will be experimentally shown that a formed deposit essentially hinders the radial fluxes of a liquid and particles.

Thus, the displacement of the three-phase contact line appears to be rather slow, and it may be stated with confidence that the external boundary of the droplet catches on the fringe; i.e., the pinning and drying of the droplet occur "at an unchanged radius." In the course of solvent evaporation, the droplet shape becomes flat (Fig. 5c) and, then, concave. At a certain moment of time (see Fig. 6), the substrate is uncovered in the center of the droplet (Fig. 5d) and the second (internal) three-phase contact line is formed. Note that thick water films on a glass surface are metastable [21]. Therefore, the aforementioned discontinuity may indicate passage to stable α-films with thicknesses of a few nanometers. However, this does not exclude the subsequent evaporation of the α-films and "uncovering" of the substrate surface. An important role in providing the film with the stability may be played by dispersed phase particles, which are adsorbed on the substrate surface (Figs. 5d–5h), and, in the case of polystyrene particles, at a liquid–gas interface [18]. These particles may also play a destabilizing role. Irrespective of the film discontinuity or the passage to the α-films, the formation of an internal boundary of the droplet is seen with an optical microscope. The internal boundary begins to be displaced from the center to the periphery ("eigendepinning") (Figs. 5e, 5f) and reaches the internal boundary of the formed fringe. Then, the internal three-phase contact line "climbs" onto the fringe and meets the external boundary of the droplet. After the droplet has dried up completely (Figs. 5g, 5h), the resulting deposit is ring-shaped.

The internal three-phase contact line arises at the final stage of the process, when the droplet has evaporated almost completely. This is seen especially clear from Fig. 6, in which the external and internal radii of a polystyrene dispersion droplet are presented as function of evaporation time. These dependences show that the displacement of the external boundary begins immediately after the droplet is applied and proceeds slowly and uniformly by a very short distance. The internal boundary is formed at nearly the 75th minute after the onset of the process and rapidly moves toward the external one from the center to the periphery.

Dispersions of Silica Particles

Absolutely different scenario is realized during the evaporation of droplets of dispersions of silica particles 255 nm in diameter. Figure 7 illustrates the stages of the evaporation of this colloidal solution droplet. Several fundamental differences from the scenario that is realized for a dispersion of polystyrene particles can be distinguished. First, after the particle is applied and the equilibrium state is established (Fig. 7a), the droplet boundary is quiescent; i.e., the pinning takes place (Fig. 8), and, during a short period of time, the evaporation occurs "at an unchanged radius," i.e., with a reduction in the contact angle. Only after a certain time delay (nearly 8 min), meniscus displacement to the center (depinning) begins (Figs 7b–7e). However, the droplet evaporates with variations in both radius and shape in this case. This is the second fundamental difference from the scenario of polystyrene dispersion

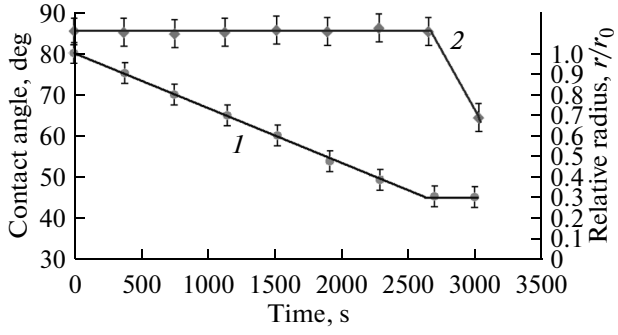

Fig. 4. Time dependences of (*1*) contact angle and (*2*) relative radius of a water droplet on a hydrophobic substrate.

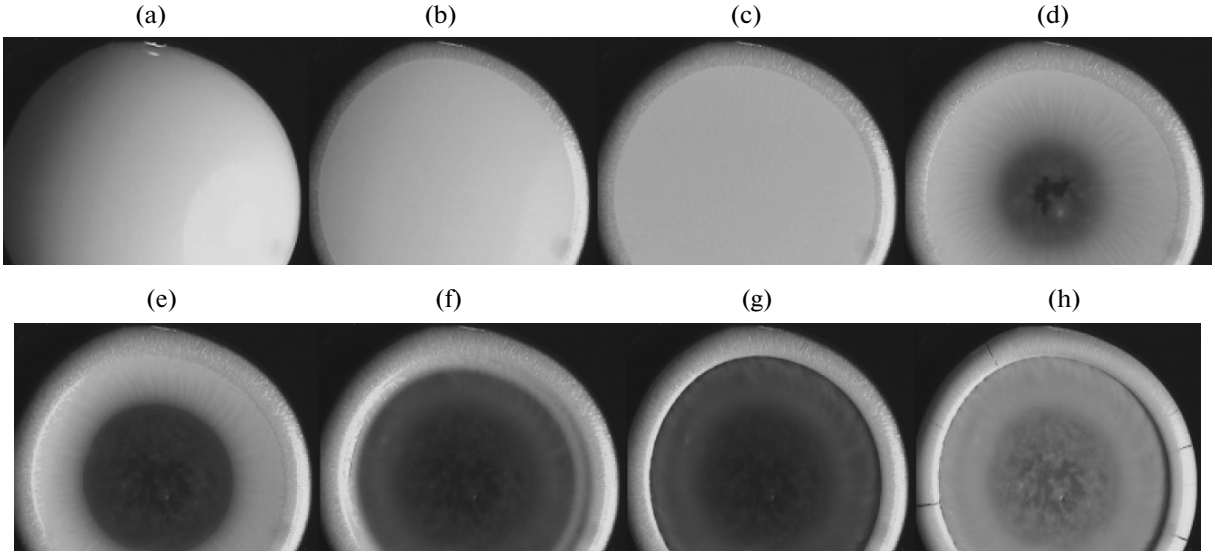

Fig. 5. Top views of an evaporating polystyrene dispersion droplet at different time moments. See text for explanations.

droplet evaporation. The third fundamental difference is that the displacement of the external boundary of the droplet to its center permanently accelerates (remember that, for the polystyrene dispersion, it decelerated). The fourth difference consists in the fact that the three-phase contact line is displaced from the periphery to the center both over the fringe and inside of it. It may be shifted from the geometric center of the fringe in a random manner for various reasons. During the displacement of the three-phase contact line, almost all particles pass from the dispersion to the solid deposit, so that the dispersion medium is actually free of particles in the zone of the final droplet evaporation (Fig. 7f), and the formation of the solid deposit stops. Obviously, this is why, immediately before the droplet disappears, the displacement of the three-phase contact line stops (pinning), while the droplet is, at an unchanged radius, transformed into a film, the evaporation of which leads to the formation of a centrally symmetric deepening in the smeared deposit spot in the internal region of the ring (Fig. 7g).

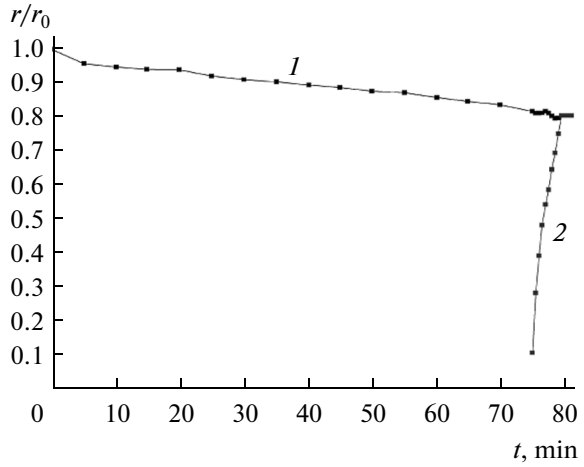

Fig. 6. Dependences of relative (*1*) external and (*2*) internal radii of a polystyrene dispersion droplet on evaporation time.

The existence of analogous stages in the two above-described scenarios should be noted. Similarly to the case of the polystyrene dispersion, the silica dispersion droplet is transformed into a film, after the disappearance of which, a substrate surface almost free of the particles emerges. However, in the case of silica dispersion droplets, this occurs very rapidly at the very end of evaporation, when the droplet size is already small. This is evident from Fig. 8, which presents the dependence of the radius of a silica dispersion droplet on evaporation time. This dependence distinctly shows the difference between the scenarios of evaporation for droplets of polystyrene and silica dispersions. As can be seen from the presented time dependence of the droplet radius, the droplet boundary is, initially, quiescent (pinning), while its displacement (depinning) begins in a certain period of time (see the horizontal region with duration of 8 min). The displacement continuously accelerates, and the final stage occurs almost instantaneously as compared with other processes. The formation of the internal three-phase contact line is, obviously, preceded by the transformation of the droplet into a small-diameter film, the perimeter of which "is anchored" and remains quiescent (pinning) until the droplet completely evaporates.

Let us pay attention to the fact that (as can be seen from Figs. 7f and 7g) the second "anchoring" of the strongly diminished droplet is preceded by the densification of the deposit in the internal region of the ring.

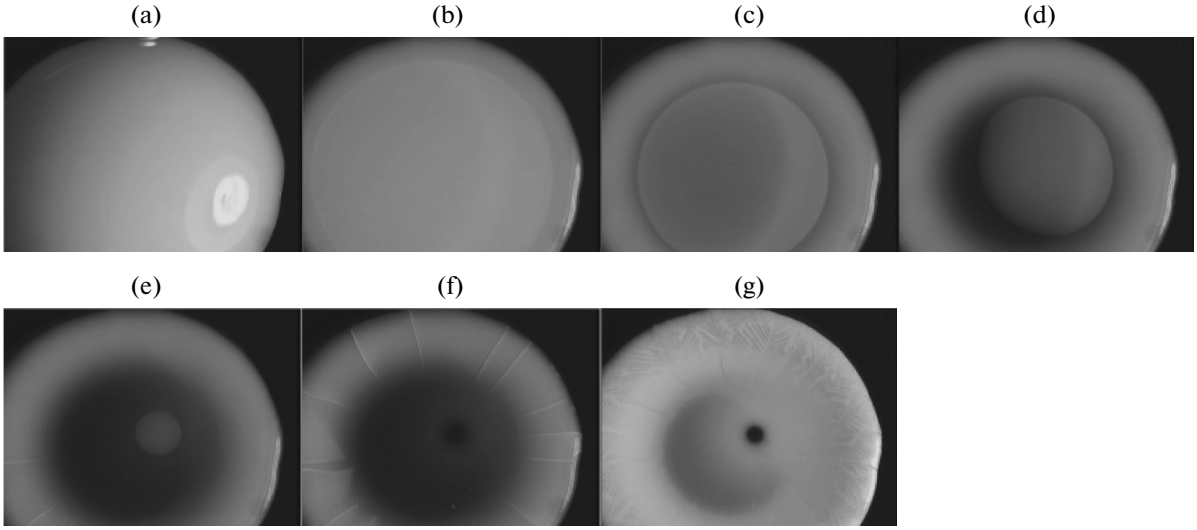

Fig. 7. Top views of an evaporating silica dispersion droplet at different time moments. See text for explanations.

This fact indicates that, in the case of small droplets, the displacement of the three-phase contact line is decelerated, thereby providing the formation of a second ring, which does not have time to acquire the thickness of the external one because of the deficiency of particles and the size factor.

In addition, the difference between the scenarios of evaporation manifests itself as different distributions of the deposit density inside the rings, which, at first sight, have the same structure. Figure 9 shows the profiles of the deposits resulting from the evaporation of droplets of polystyrene and silica dispersions. The attentive consideration thereof testifies that the external deposit rings, which have similar shapes, are fundamentally different. The deposit of silica particles has a larger width and a smaller height than the deposit of polystyrene particles has (note that the volume of the particles in the deposits is almost the same). Thus, it seems that the polystyrene deposit grows upward, while the silica deposit widens.

The structures of the secondary deposits are also essentially different. In the case of polystyrene particles, the secondary ring-shaped deposit adjoins the main ring, while silica particles form it in the central region of an evaporating dispersion droplet.

The observed profiles completely agree with the above-described characters of the evaporation of the dispersion droplets.

More substantial differences are observed in the case of evaporating droplets of SiO_2 nanoparticles of the Levasil brand, which we are starting to consider.

Dispersions of Levasil Nanoparticles

Figure 10 illustrates the stages of the evaporation of a Levasil nanoparticle dispersion droplet. In this case, the three-phase contact line remains quiescent for a long time (as long as 90 min) (Figs. 10a, 10b); i.e, pinning takes place. Therewith, the curvature radius of the droplet surface increases, while the contact angle decreases; that is, the evaporation proceeds via the scenario "at an unchanged radius." After this time elapses, the external boundary of the droplet starts moving toward the center (Figs. 10c, 10d), leaving an almost even layer of the solid deposit after itself. Thus, the droplet evaporates via the scenario "at an unchanged shape." When the droplet leaves the solid deposit, drying up of deposit edges begins, which leads to their cracking and, then, to peeling from the substrate and deformation. This indicates a great shrink-

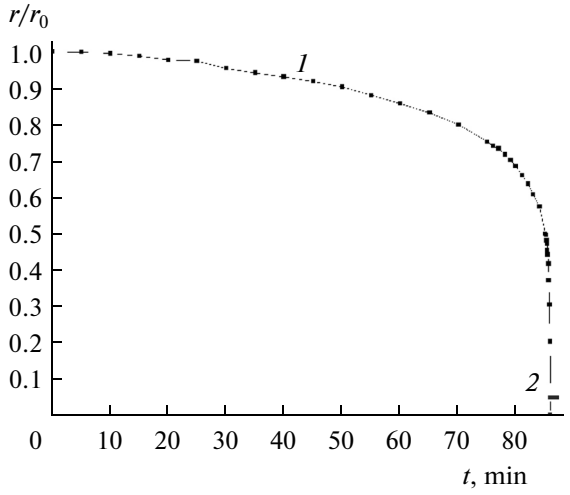

Fig. 8. Time dependences of (*1*) external and (*2*) internal radii of a silicon dioxide dispersion droplet. Horizontal line denotes the particle-free circular region in the central part of the deposit (see Fig. 7g).

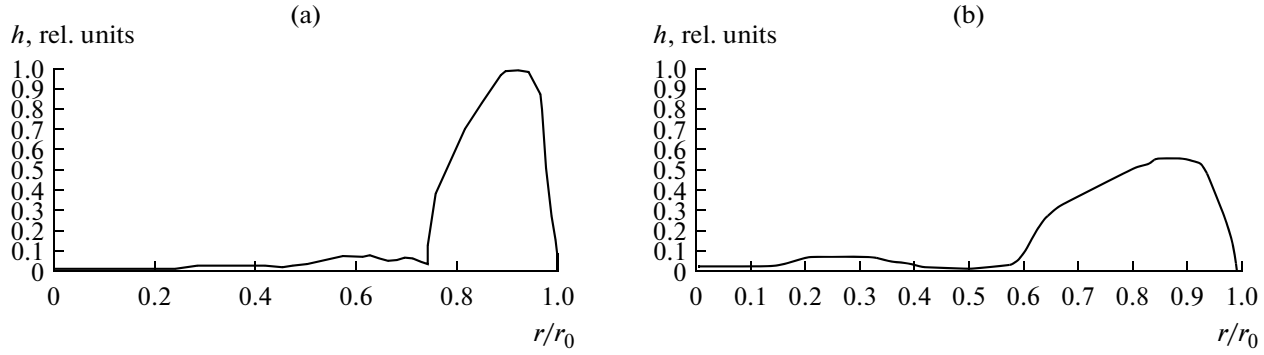

Fig. 9. Distributions of deposit height h over radius for droplets of (a) polystyrene and (b) silica dispersions.

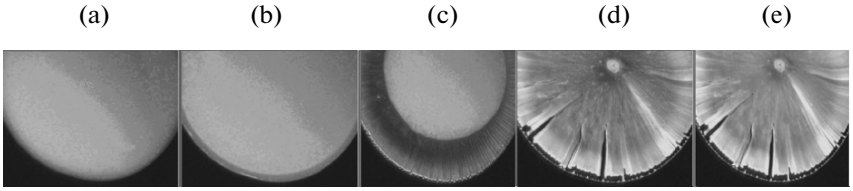

Fig. 10. Top views of an evaporating Levasil dispersion droplet at different time moments. See text for explanations.

age of the formed disk-shaped deposit in the course of its drying. As the sizes of the droplet decrease, the disk edges rise to form a structure similar to a folding flower bud. The droplet diminishes in size and completely disappears via collapsing toward the center of the deposit. After the droplet disappears and the solid deposit completely dries, the formed structure disintegrates (Fig. 10e). Nevertheless, the deposit has the shape of a fragmented, but smooth, disk.

The time dependence of the droplet radius is shown in Fig. 11. In contrast to droplets of other dispersions, a longer induction period is, in this case, observed, after which the size of the droplet begins to dramatically decrease. The data presented in Figs. 10 and 11 clearly show that the scenario of the evaporation of the Levasil nanoparticle suspension droplets and the structure of the formed deposit fundamentally differ from those taking place in the two previous cases. This suggests that the structure of a deposit and the nature of the particles composing it rather strongly affect the character of droplet evaporation; i.e., the behavior of a dispersion in the region of the meniscus is the dominant factor.

RESULTS AND DISCUSSION

The aforementioned data indicate that three different scenarios of dispersion droplet evaporation may be distinguished for the systems under investigation, with each of them having its characteristic features.

I. Evaporation from the center to the periphery with the formation of a ring-shaped deposit.

II. Evaporation from the periphery to the center with the formation of a ring-shaped deposit.

III. Evaporation from the periphery to the center with the formation of a disk-shaped deposit.

The scenarios differ in not only the structure of the deposit and the direction of the displacement of the three-phase contact line, but also the durations of the periods of time from the moment of droplet application to the onset of the contact line displacement (depinning time) and the contact angle at which it takes place (depinning angle). The values of these parameters correlate with each other: the smaller the angle the longer the period.

It is useful to present the data on the initial contact angles of the studied droplets, depinning angles, and times of depinning onset. The corresponding parameters for dispersion droplets of polystyrene, silica, and Levasil, which are summarized in the table, indicate that, for all dispersions, the initial contact angles are equal within the experiment error; i.e., at a fundamental level, the droplets have the same shapes and sizes. However, an obvious difference is observed in the values of the depinning angle and time.

Still more essential differences take place in the regularities of variations in the shapes of the droplets. According to scenario I, the external boundary of the droplet does not leave the main ring-shaped deposit, the convex droplet surface is transformed into, initially, a flat and, then, a concave one; further, after the rupture of the film in the center and the formation of the internal meniscus, the droplet is transformed into a torus. In accordance with scenario II, the external boundary of a droplet is gradually displaced into the

inside of the ring-shaped deposit, while the convex shape remains preserved up until the point at which the droplet collapses into a point (in the scale of the external deposit). Only at the final stage, when the sizes of the droplet become very small, is it transformed into a film, at which point it rapidly disappears. According to scenario III, the external boundary of the droplet is displaced along the formed disk-shaped deposit from the periphery to the center, with the droplet shape remaining convex all the time.

Note that, in [19], only two scenarios similar to the first and second ones were described and explained based on the substantial difference in the receding angles of dispersions on a smooth substrate formed from the particles. In the author's opinion, the reason for depinning was the fulfillment of one of the following conditions: reaching of either the limiting concentration of particles, which corresponds to the dense packing thereof, or the limiting receding angle on the formed deposit. Moreover, it was assumed that, as soon as compensatory fluxes inside the droplet deliver a sufficient amount of particles to the three-phase contact line and arrange them into a dense structure, this line is displaced along the deposit climbing onto it. Therewith, the droplet perimeter is retained by the edge of the formed deposit, its displacement beginning only when the contact angle decreases to a value corresponding to the receding angle. According to this scheme, at large and small receding angles, the droplet evaporates "from the periphery to the center" (scenario II) and "from the center to the periphery" (scenario I), respectively.

Our data indicate that this scheme does not agree with reality. The character of the three-phase contact line displacement and the data presented in the table and Figs. 6, 8, and 11 attest to the opposite situation: at a large depinning angle, the three-phase contact line "is anchored" to the external deposit ring and the first scenario is realized; at smaller angles, it is displaced to the center of the contact spot (scenarios II and III).

The data in the table seem to indicate that the reason for the realization of different scenarios is, nevertheless, different values of the angle and depinning time. Let us substantiate this statement.

In the case of polystyrene particles, the displacement of the three-phase contact line begins immediately after the droplet application at a large contact angle (31°). Accordingly, a deposit with a steep profile is formed, because it reproduces the current profile of the droplet; therefore, its "construction" requires a large specific number of particles (per unit substrate surface). The presence of particles at the liquid–gas interface may play an important role in the construction of the deposit. This is the case for polystyrene particles, because, as was mentioned in [18], the particles are adsorbed on water surface. In the case of silica particles, the displacement of the three-phase contact line is preceded by a time pause (8 min) caused by a smaller depinning angle (26°), with the droplet profile becoming flatter during this pause. Therefore, the deposit profile appears to be flatter as well. In this case, the negative adsorption of silica particles may also play a certain role (see [18]). It is obvious that the construction of a deposit with a flatter profile requires a substantially smaller specific amount of particles. At the same rate of solvent evaporation, the processes of deposit formation and three-phase contact line displacement are faster for the silica dispersion, while the consumption of particles for the formation of the deposit is lower. In the case of polystyrene dispersions, the specific consumption of particles is higher, which brings about a lower rate of meniscus displacement and its subsequent cessation because of lack of particles.

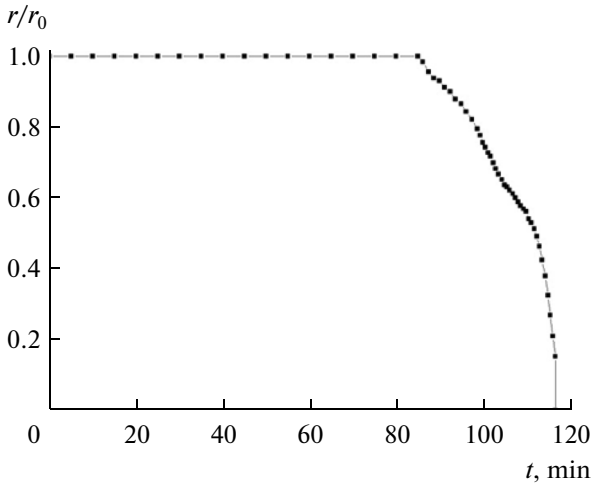

Fig. 11. Radius of a Levasil dispersion droplet as a function of evaporation time.

Since the particle concentration in a droplet decreases with time, at a certain stage, the deposit ceases to grow and the main peripheral ring is formed.

In the case of Levasil dispersions, the depinning angle has the smallest value. Therefore, the droplet perimeter remains quiescent for a long time, while the shape of the droplet continuously varies; i.e., its curvature radius increases. The compensatory fluxes transfer nanoparticles to the wetting line, thereby continuously maintaining their concentration at the limiting level.

However, the deposit initially formed in the region of the meniscus has a low strength; therefore, nanoparticles can be "squeezed out" by the capillary forces toward the droplet center, thereby leveling the thickness of the ring-shaped deposit during the displacement of the three-phase contact line. Accordingly, after the onset of the depinning, only the width of the ring-shaped deposit grows along the substrate surface. The low consumption of the particles predetermines the maintenance of a high bulk concentration thereof and the continuous displacement of the meniscus. As

a result, a deposit having the shape of an almost regular flat disk is formed.

Thus, the presented results lead us to conclude that the existence of the three scenarios of the formation of deposits as a result of the evaporation of dispersion droplets may be explained by different depinning angles of droplets and properties of deposits. This suggests that the effects of the pinning and depinning should be studied more profoundly. However, it may now be stated that the existing ideas of the reasons for depinning must be revised. For example, reaching the limiting concentration of particles in a solution at the three-phase contact line is not the reason for depinning. A striking example is the dispersion of Levasil particles, the perimeter of which remains quiescent for 90 min. The necessity to revise the causes of depinning is also evident from the behavior of polystyrene and silica particle dispersions, for which the attainment of the critical angle is not always accompanied by depinning.

Secondary features of each scenario that were only observed in experiments that we performed under certain conditions should be noted. Let us indicate them as being related to the above-introduced scenarios.

I-1. Formation of a second ring adjacent to the main one.

II-1. Formation of a separate second ring.

III-1. Strong cracking and pilling of the deposit formed as a monolithic disk.

Let us briefly consider these peculiarities.

In the case of polystyrene dispersions, the deposit being formed retains the droplet meniscus. After the droplet is transformed into a film and the latter is ruptured, an internal meniscus is formed in the center of the droplet and begins to move from the center to the periphery of the droplet. A deposit is also formed on the internal meniscus, while the compensatory fluxes carry the particles from the main ring to the central region of the droplet. As a result, the second ring separated from the main one with a zone depleted with particles is formed.

The second ring is also formed upon the deposition of silica particles. In this case, the droplet is flattened and the meniscus is displaced with the formation of a thin deposit layer. As the dispersion is depleted with particles, the growth of the external "thick" ring begins not to keep pace with the meniscus displacement and it goes down to the internal region of the ring. The droplet volume decreases in the course of evaporation. According to the rough approximation [1], the evaporation rate may be considered to be constant. At the same time, the flux of the droplets to the periphery (perimeter) of the droplet decreases with the droplet size, because it is proportional to the perimeter length. Therefore, an increase in the particle concentration in the droplet and a relevant thickening of the deposit are observed. The deposit thickening causes deceleration of the displacement of the three-phase contact line, which, in turn, still more enhances the transfer of particles to the region of the meniscus an the accumulation thereof in this region. Thus, a small second ring arises inside the large one, but it cannot reach the thickness of the large ring because of the deficiency of particles.

Under certain conditions, this deceleration of the three-phase contact line displacement leads to the formation of a deposit with a many-ring structure. Detailed analysis of the reasons and conditions for the formation of these structures will be the subject of a separate communication.

The cracking of a disk-shaped deposit of Levasil nanoparticles is obviously explained by its loose structure and the shrinkage caused by the evaporation of bound water. While the deposit dries, it is dehydrated from above to below and from the periphery to the center in the course of the three-phase contact line displacement. Radial cracks grow in the deposit during its dehydration from the periphery to the center. At the same time, internal stresses that develop while the deposit is dehydrated from above to below peel the formed segments of the deposit from the substrate and impart a concave shape to them. This behavior of the deposit is only inherent in the Levasil dispersions and is not observed for other systems.

Now, let us compare the behaviors of evaporating droplets of pure water and dispersions. In the case of a hydrophilic substrate, with which water strongly interacts, wetting hysteresis is observed as the initial pinning (Figs. 1, 2), which leads to the droplet evaporation "at an unchanged radius." The interaction of water with a hydrophobic substrate is weak, the wetting hysteresis is almost absent, and the meniscus is displaced, thereby causing the droplet to evaporate "at an unchanged shape" (Figs. 3, 4). Further, let us consider the droplets of the dispersions. In the case of the Levasil dispersion, a strong bonding takes place between the droplet liquid and the deposit, which is evident from the small depinning angle; however, the external boundary of the droplet is displaced from the periphery to the center, and the droplet evaporation from the periphery to the center takes place "at an unchanged shape," which is typical of the weak bonding. In the case of the polystyrene dispersion, a weak bonding between a droplet and a deposit takes place, which manifests itself as a small depinning angle; however, the external boundary of the droplet remains quiescent until the liquid is completely evaporated (drying "at an unchanged radius"), which is typical of a strong bonding. A droplet of the silica dispersion also exhibits an "abnormal" behavior. Judging by the depinning angle, the bonding between the dispersion and the deposit is much stronger than that in the case of polystyrene particles. However, the external boundary is not retained by the ring-shaped deposit, while the droplet evaporates with variation in the radius (evaporation "at both radius and shape being changed"). All of the aforementioned once again confirms that the regularities of

deposit formation and meniscus displacement are rather complex and contradict simple considerations, thereby indicating that the processes occurring in the region of the menisci of evaporating dispersion droplets are to be studied in greater detail.

CONCLUSIONS

The above-presented results show that the formation of ring-shaped deposits during the evaporation of dispersion droplets is a rather complex multistage process. The common ideas of the formation of a deposit dense structure and the displacement of the three-phase contact line along a substrate do not enable one to predict all regularities of CRE. At least three fundamentally different scenarios may be distinguished between, with each of them being characterized by its own processes that affect meniscus displacement and deposit formation. The main scenarios are as follows.

(1) Droplet evaporation from the center to the periphery with the formation of a ring-shaped deposit.

(2) Droplet evaporation from the periphery to the center with the formation of a ring-shaped deposit.

(3) Droplet evaporation from the periphery to the center with the formation of a disk-shaped deposit.

Each scenario is characterized by not only the shape of a deposit, but also its own duration of the pinning of the meniscus, character of its displacement, and the value of the depinning contact angle. All these parameters and the structure of a deposit essentially depend on the nature of dispersion particles, which, in the long run, predetermines the scenario of CRE manifestation.

REFERENCES

1. Fuks, N.A., *Isparenie i rost kapel' v gazoobraznoi srede* (Drop Evaporation and Growth in Gaseous Medium), Moscow: Akad. Nauk SSSR, 1958.
2. Loyalka, S.K., *Prog. Nucl. Energy*, 1983, vol. 12, p. 1.
3. Williams, M.M.R. and Loyalka, S.K., *Aerosol Science: Theory and Practice,* Oxford: Pergamon, 1991.
4. Erbil, H.Y., *Adv. Colloid Interface Sci.*, 2012, vol. 170, p. 67.
5. Kawase, T., Sirringhaus, H., Friend, R.H., and Shimoda, T., *Adv. Mater.* (Weinheim, Fed. Repub. Ger.), 2001, vol. 13, p. 1601.
6. Roldughin, V.I., *Usp. Khim.*, 2004, vol. 73, p. 123.
7. Dugas, V., Broutin, J., and Souteyrand, E., *Langmuir*, 2005, vol. 21, p. 9130.
8. Saverchenko, V.I., Fisenko, S.P., and Khodyko, Yu.A., *Colloid J.*, 2015, vol. 77, p. 71.
9. Deegan, R.D., Bakajin, O., Dupont, T.F., Huber, G., Nagel, S.R., and Witten, T.A., *Nature* (London), 1997, vol. 389, p. 827.
10. Deegan, R.D., Bakajin, O., Dupont, T.F., Huber, G., Nagel, S.R., and Witten, T.A., *Phys. Rev. E: Stat. Phys., Plasmas, Fluids, Relat. Interdiscip. Top.*, 2000, vol. 62, p. 756.
11. Sefiane, K. and Bennacer, R., *Adv. Colloid Interface Sci.*, 2009, vols. 147–148, p. 263.
12. Sefiane, K. and Bennacer, R., *J. Fluid Mech.*, 2011, vol. 667, p. 260.
13. David, S., Sefiane, K., and Tadrist, L., *Colloids Surf. A*, 2007, vol. 298, p. 108.
14. Vysotskii, V.I., Roldughin, V.I., Uryupina, O.Ya., and Zaitseva, A.V., *Colloid J.*, 2011, vol. 73, p. 176.
15. Vysotskii, V.V., Uryupina, O.Ya., Senchikhin, I.N., and Roldughin, V.I., *Colloid J.*, 2013, vol. 75, p. 142.
16. Vysotskii, V.V., Uryupina, O.Ya., Senchikhin, I.N., and Roldughin, V.I., *Colloid J.*, 2013, vol. 75, p. 634.
17. Vysotskii, V.V., Roldughin, V.I., Uryupina, O.Ya., Senchikhin, I.N., and Zaitseva, A.V., *Colloid J.*, 2014, vol. 76, p. 531.
18. Molchanov, S.P., Roldughin, V.I., and Chernova-Kharaeva, I.A., *Colloid J.*, 2015, vol. 77, p. 761.
19. Bhardwaj, R., Fang, X., and Attinger, D., *New J. Phys.*, 2009, vol. 11, p. 075020.
20. Lebedev-Stepanov, P.V., Kadushnikov, R.M., Molchanov, S.P., Rubin, N.I., Shturkin, N.A., and Alfimov, M.V., *Nanotechnol. Russ.*, 2010, vol. 5, nos. 11–12, p. 83.
21. Derjaguin, B.V. and Churaev, N.V., *Smachivayushchie plenki* (Wetting Films), Moscow: Nauka, 1984.

Translated by A. Kirilin